Journal of Magnetic Resonance 194 (2008) 283–288

Contents lists available at ScienceDirect

Journal of Magnetic Resonance

journal homepage: www.elsevier.com/locate/jmr

Spin-diffusion couples proton relaxation rates for proteins in exchange with a membrane interface

Anshu Bhowmik, Jeffrey F. Ellena, Robert G. Bryant *, David S. Cafiso *

Department of Chemistry and Biophysics Program, The University of Virginia at Charlottesville, P. O. Box 400319, Charlottesville, VA 22904-4319, USA

ARTICLE INFO

Article history:
Received 3 June 2008
Revised 17 July 2008
Available online 3 August 2008

Keywords:
Spin-diffusion
Cross-relaxation
Spin temperature
C2 domain
Lipid bilayer
Paramagnetic enhancement

ABSTRACT

Changes in nuclear spin-lattice relaxation rates that are induced by a freely diffusing paramagnetic relaxation agent are examined for a protein in solution and compared to the case where the protein binds to a membrane. In the solution case, the intramolecular cross-relaxation rates are modest and large differences are observed in the oxygen induced protein–proton relaxation rates. In the case where a dynamic equilibrium between solution and membrane-bound environments is established, the intramolecular ^{1}H cross-relaxation rates for the protein protons increase dramatically because of the slow reorientational motion in the membrane-bound environment. As a consequence, all protein protons relax with nearly the same spin-lattice relaxation rate constants when bound to the membrane, and site specific relaxation effects of the diffusing paramagnet are suppressed. Slowly reorienting sites or rotationally immobilized sites sampled by observable molecules in vivo will demonstrate similar relaxation leveling effects.

1. Introduction

The reversible association of proteins with membranes plays a critical role in cell-signaling and membrane trafficking within cells, and the importance of this association is underscored by the fact that the majority of the domains found in soluble proteins are membrane binding domains [1]. High-resolution models for the docking and association of proteins with membrane interfaces can provide information on the forces that control membrane-protein association, but these models are often difficult to generate. At the present time, a number of approaches have been used to determine orientation and penetration of proteins at the membrane-solution interface, including site-directed spin labeling [2], fluorescence [3], X-ray reflectivity [4], and infra-red spectroscopy [5].

Nuclear magnetic resonance spectroscopy provides a powerful method for protein structure determination. The use of a paramagnetic co-solute, which produces an enhancement in nuclear relaxation, can also provide information on intermolecular association and residue accessibility [6–19]. For a freely diffusing paramagnetic species, nuclear spins are relaxed at a rate that is related to distances of closest approach and time averaged collisional access to nuclear spins. For example, if the paramagnet does not penetrate the structure, the different relaxation enhancements will identify spins that are accessible or close to the surface of the folded macromolecule. If there is a protein–protein association or a membrane-protein association, the accessibility of the paramagnetic agent to the interfacial protons will be altered, changing the relaxation rate constants and defining the surface involved in the interaction. Nevertheless, membrane environments pose significant additional spectroscopic challenges because of line-broadening that results from the slow rotational reorientation of the membrane-bound protein. The membrane represents one class of bound environments available in vivo that may also cause major broadening of NMR spectra of a molecule that samples the relatively immobilized state.

When a protein associates with a membrane, NMR spectral resolution is lost because the effective correlation time for the internuclear dipolar coupling, which determines the linewidth, is increased by more than a factor of 100. This problem may be circumvented if a dynamic equilibrium is established between the membrane environment and the solution phase. In this case, the exchange averaged NMR linewidth can be reduced and a high resolution spectrum recovered. If the chemical exchange between the membrane and solution environments is fast, information about the protein in the membrane environment may be transferred to and detected in the solution environment. These conditions are relatively easy to satisfy for spin-lattice relaxation time constants, which are on the order of tenths of seconds. In the fast exchange limit, the observed relaxation rate constant $1/T_1$ is the weighted average,

$$\frac{1}{T_1} = \frac{P_M}{T_{1M}} + \frac{P_S}{T_{1S}}, \tag{1}$$

* Corresponding authors. Fax: +1 434 924 3567.
E-mail addresses: rgb4g@virginia.edu (R.G. Bryant), cafiso@virginia.edu (D.S. Cafiso).

1090-7807/$ - see front matter © 2008 Elsevier Inc. All rights reserved.
doi:10.1016/j.jmr.2008.07.023

where P_M and P_S are the probabilities that the protein is bound to the membrane or in solution with relaxation times T_{1M} and T_{1S}, respectively. If the membrane-bound fraction of protein is not large, the spectral resolution is retained, and information on the membrane environment of the protein may be obtained from the perturbation of the solution phase spectrum caused by the membrane-bound population.

A water-soluble paramagnetic relaxation agent should produce nuclear relaxation enhancement for both the solution phase and membrane-bound protein. However, the relaxation efficiency may differ between the two environments because of different effective concentrations, accessibility, and dynamics that control the relaxation rate changes. If the paramagnetic species is molecular oxygen, it is well-known that oxygen solubility in hydrocarbon is high relative to water [20] and that there is an oxygen concentration gradient in the lipid bilayer with a maximum concentration near the bilayer center [16,17,21]. Because of its higher solubility in the bilayer, the effect of oxygen on the protein spins when bound to the membrane would be expected to be largest for that portion of the protein that is inserted into the membrane. As a result, the relative relaxation rate enhancements would encode information protein orientation on membrane depth as well as hydrocarbon exposure. In this case, this general approach may provide useful information about how the protein inserts into the membrane. However, we show below that this general approach is strongly affected by changes in the spin-dynamics in the membrane bound-protein.

We investigate here the membrane interactions of a soluble Ca^{2+}-dependent membrane binding domain (C2A) from synaptotagmin 1 (syt1C2A). Synaptotagmin I has been identified as the calcium ion sensor in neuronal exocytosis [22,23], and syt1C2A is the first C2 domain in synaptotagmin 1 encompassing residues 140–265. The syt1-C2A domain associates with phospholipid membranes containing phosphatidylserine (PS) in the presence of calcium ion, and site-directed spin labeling studies have shown that residues in the calcium binding region of the domain interact preferentially with the lipid to a depth of approximately 5 Å [24]. The membrane binding affinity may be controlled by altering the composition of the phospholipid and the calcium level in the solution, and sytIC2A provides a convenient system to test the use of an NMR exchange experiment to map protein–membrane interactions.

2. Methods

2.1. Materials

1-Palmitoyl-2-oleoyl-sn-glycero-3-phosphocholine (POPC) and 1-palmitoyl-2-oleoyl-sn-glycero-3-phosphotidylserine, (POPS) were purchased from Avanti Polar Lipids, Inc. (Alabaster, AL). *Escherichia coli* BL21(DE3) plysS bacterial cells were obtained from Promega Corporation (Madison, WI). Nitrogen-15 ammonium sulfate, $(^{15}NH_4)_2SO_4$, (98% pure), deuterium oxide, D_2O (99.9% pure) and perdeuterated acetate, CD_3COONa (98% pure) were purchased from Cambridge Isotopes, Inc. (Andover, MA). GSTrap FF pre-packed columns, benzamidine pre-packed columns, Hiprep desalting columns and thrombin protease (500 U) were obtained from Amersham Biosciences (Piscataway, NJ). High fidelity Vent DNA polymerase and all restriction endonucleases were obtained from New England Biolabs (Beverly, MA). Isopropyl-β-D-thio-galactopyranoside, IPTG, was obtained from Roche Diagnostics Corporation, Inc. (Indianapolis, IN).

2.2. Expression and purification of synaptotagmin I C2A domain

The first C2 domain (C2A) of rat synaptotagmin I (SYTI) was expressed as a recombinant fusion protein with Glutathione-S-transferase (GST), [SYTI C2A-GST fusion protein]. To produce the necessary plasmid, the gene encoding residues 136–265 (~17.4 KDa) from the wild type C2A domain was ligated into the plasmid vector pGEX-kG following the coding region for GST. The recombinant plasmid was transformed into *E. coli* BL21(DE3) plysS bacterial cells.

Protein was expressed and purified as described previously [25], with the following modifications. The pre culture (grown in Luria–Bertani (LB) media) was used to inoculate a 50 mL minimal media pre culture and grown for 8–10 h at 37 °C. This pre culture was then used to incubate a 1 L culture of minimal media having $(^{15}NH_4)_2SO_4$ as the sole nitrogen source. The minimal media contained 10.5 g K_2HPO_4, KH_2PO_4, 1 g $(NH_4)_2SO_4$, 0.5 g Na-citrate, along with 3 mM $MgSO_4$, 0.3 mM $CaCl_2$ and glucose 0.2% (w/v), per liter. All media contained 50 mg/mL ampicillin. The purity of the C2A domain was determined by SDS–PAGE (Bio-Rad, Inc., Hercules, CA) and molecular weight was confirmed by mass spectrometry (Biomolecular Research Facility, University of Virginia, VA). The molecular weight for SYTI C2A was approximately 17.4 kDa, and included residues 136–265 and 10 additional residues from the pGEX vector each on the N- and C-terminus of the C2A domain.

2.3. NMR sample preparation

All NMR samples for the solution measurements were made in an NMR buffer containing 9:1 H_2O:D_2O with 100 mM NaCl, 40 mM CD_3COONa, and 5 mM $CaCl_2$ pH 5.0. The buffer was added directly to the pre-weighed lyophilized protein and the pH of the sample was adjusted. For the lipid measurements, Small Unilamellar Vesicles (SUV's) were prepared as follows. NMR buffer without Ca^{2+} was first added to a dried mixture of POPC and POPS (lipids were mixed in chloroform in a ratio of 95:5 POPC:POPS and dried under nitrogen, followed by drying 8–12 h under vacuum). The hydrated lipid mixture was subjected to micro-tip sonication on ice for about 15 min under N_2. The lipid sample was then centrifuged at 40,000g to remove particulates. $CaCl_2$was added to the lipid mixture slowly to avoid any precipitation. The final lipid preparation was then added to the lyophilized C2A domain and the pH adjusted. The protein solution was degassed of any dissolved air with 5–6 freeze-thaw cycles, and pressurized under 10 atm O_2 or N_2. Protein concentrations for NMR spectroscopy were approximately 1–1.2 mM with a lipid concentration of 25 mM. The NMR samples were placed in High Pressure NMR tubes (Wilmad Labglass, Inc., Buena, NJ).

2.4. NMR spectroscopy

A Varian Inova 500 NMR spectrometer and a modified Varian Biopack gNhsqc pulse sequence were used to obtain ^{1}HN spin-lattice relaxation rates (R_1) via the saturation recovery method. Two ^{1}H 90° pulse, magnetic field gradient pairs were added to the beginning of the gNhsqc sequence, analogous to the ^{15}N 90° pulse magnetic field gradient pairs at the beginning of the original gNhsqc sequence.

Proton relaxation rate constants were measured for uniformly backbone ^{15}N-labeled Ca^{2+} bound SYTI C2A in samples where the lipid composition was adjusted to provide a labile protein exchange between the solution and the membrane environment at pH 5.0. The paramagnetic contribution to the relaxation rate constants was determined from the difference between measurements in the presence of 10 atm oxygen and 10 atm nitrogen.

$$\Delta R_{1,\mathrm{PRE}} = \frac{1}{T_{1,\mathrm{PRE}}} = \frac{1}{T_1^{O_2}} - \frac{1}{T_1^{N_2}} \tag{2}$$

^{15}N and ^{1}H chemical shift assignments for the Syt1C2A domain in the Ca^{2+}-bound form at pH 5.0 were taken from the Bio Magnetic Resonance Bank (BMRB 4041).

The cross-peak intensities of each individual backbone amide proton obtained at the delay times 0.1, 0.2, 0.3, 0.4, 0.6, 0.8, 1.0, 1.2, 1.6, 2.0, 2.4, and 2.8 s and were fit to the single exponential:

$$I(t) = B + I(\infty)(1 - e^{tR_1}) \quad (3)$$

where $I(t)$ is the cross peak intensity measured at delay time t, $I(\infty)$ is the maximum intensity at the infinite delay time, R_1 is the spin-lattice relaxation rate constant, $1/T_1$, and B accounts for incomplete saturation.

3. Results and discussion

The binding of the C2A domain of synaptotagmin 1 (sytC2A) to membranes is Ca^{2+}-dependent. In the presence of Ca^{2+}, sytC2A binds to POPC:POPS (3:1) bilayers with an affinity of approximately 1 mM (Kuo and Cafiso, unpublished). The NMR exchange experiment requires conditions of lipid composition and protein concentration where the majority of the sytIC2A domain is in solution but in equilibrium with a minor population of protein that is bound and dilute on the membrane surface. Because of the relatively high concentrations of C2A that are required for the NMR experiment (on the order of 1 mM), membranes containing 3:1 POPC:POPS could not be used, and a series of POPC:POPS concentrations were explored that would allow high solution concentrations of C2A, but result in a small fraction of membrane-bound protein.

EPR spectroscopy was used to determine the membrane-aqueous equilibrium of the C2A domain as a function of lipid (POPS) composition. Shown in Fig. 1a is the solution structure (PDB ID:1-BYN) of the syt I C2A domain. This protein was mutated to cysteine at a single site in the first Ca^{2+} binding loop (L1), and then derivatized with a sulfhydryl-reactive spin label to replace the methionine at position 173 with the spin-labeled side chain R1, as described previously (Fig. 1b) [25]. The EPR spectrum at this site is sensitive to membrane association of the domain (Fig. 1c) and was used to measure the membrane-aqueous partitioning of sytC2A as described previously [26]. The EPR spectrum indicates that at a POPC:POPS ratio of 95:5, approximately 5% of sytC2A is membrane associated when 25 mM total lipid is present.

In addition to lipid composition, we explored broadening in the NMR spectra as a function of lipid concentration at a fixed ratios of POPC:POPS. Shown in Fig. 2 are HSQC spectra recorded with increasing lipid concentration at a lipid composition of POPC:POPS (95:5). At a lipid concentration of 25 mM, the HSQC spectra are well-resolved; however, increases beyond this concentration result in a significant broadening and loss in cross-peak intensities making accurate T_1 measurements problematic. A practical dynamic equilibrium between bound and unbound C2A domain was found for samples containing approximately 1 mM protein and 25 mM lipid with a composition of 95:5 POPC:POPS. This composition yields a coverage of sytC2A on the external surface of the vesicle of approximately one protein per 250 lipids.

Relaxation rate constant measurements in the presence of nitrogen are shown in Fig. 3 for sytC2A both in solution and in the presence of lipid vesicles. At most residue positions, the relaxation rates in the presence and absence of membranes are similar, with small but significant increases in relaxation rates at most sites for the membrane-bound case. Given that approximately 5% of the protein is associated with the membrane, small changes are expected.

Fig. 4 shows the paramagnetic enhancements in sytC2A produced by molecular oxygen in solution and in the presence of POPC:POPS bilayers. In solution (open symbols), oxygen enhancements are elevated, and there is a significant variation in the effect of oxygen on relaxation rates along the polypeptide chain. A three-dimensional representation of these rates on the C2A domain structure is shown in Fig. 5a. These variations are somewhat complex, and they are not correlated with the proximity of the amid protons to the hydrated protein surface. These variations may reflect very weak binding interactions of oxygen at different positions, in addition to differences in oxygen accessibility caused by the steric factors created by the protein fold [27]. They will not be analyzed in detail here. In the presence of POPC:POPS vesicles, the oxygen effects on the protein spins are strikingly different (solid symbols in Fig. 4). Fig. 5b shows these rates mapped onto the C2A domain structure. In general, the relaxation rate changes induced by oxygen in the presence of membranes are smaller and the site-specific differences noted above are largely eliminated.

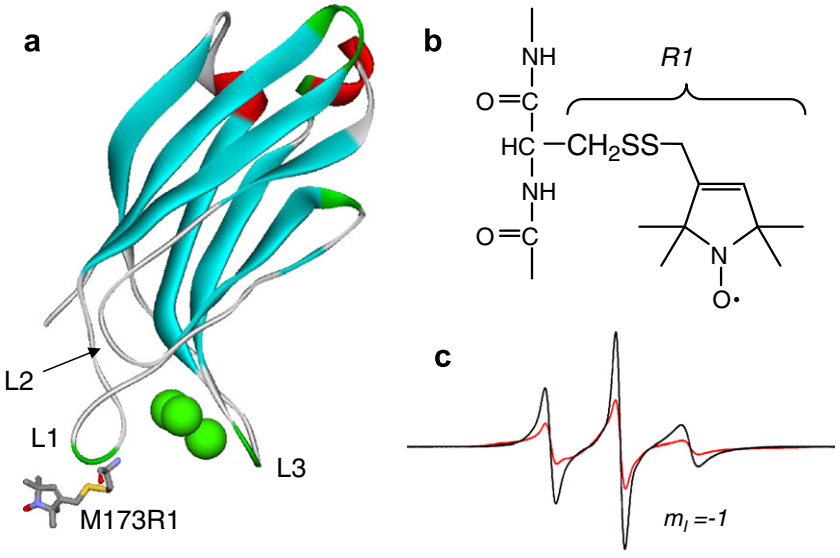

Fig. 1. (a) Solution NMR structure of synaptotagmin 1 C2A (PDB ID: 1BYN), showing the three Ca^{2+} ions (green), and the three Ca^{2+}-binding loops. EPR was used to estimate the binding affinity to the protein with the spin label liked to position 173 in the first Ca^{2+}-binding loop. (b) Structure of the spin labeled side-chain R1. (c) X-band EPR spectra of M173R1 in buffer, and fully associated with POPC:POPS (3:1) bilayer using saturating calcium ion levels.

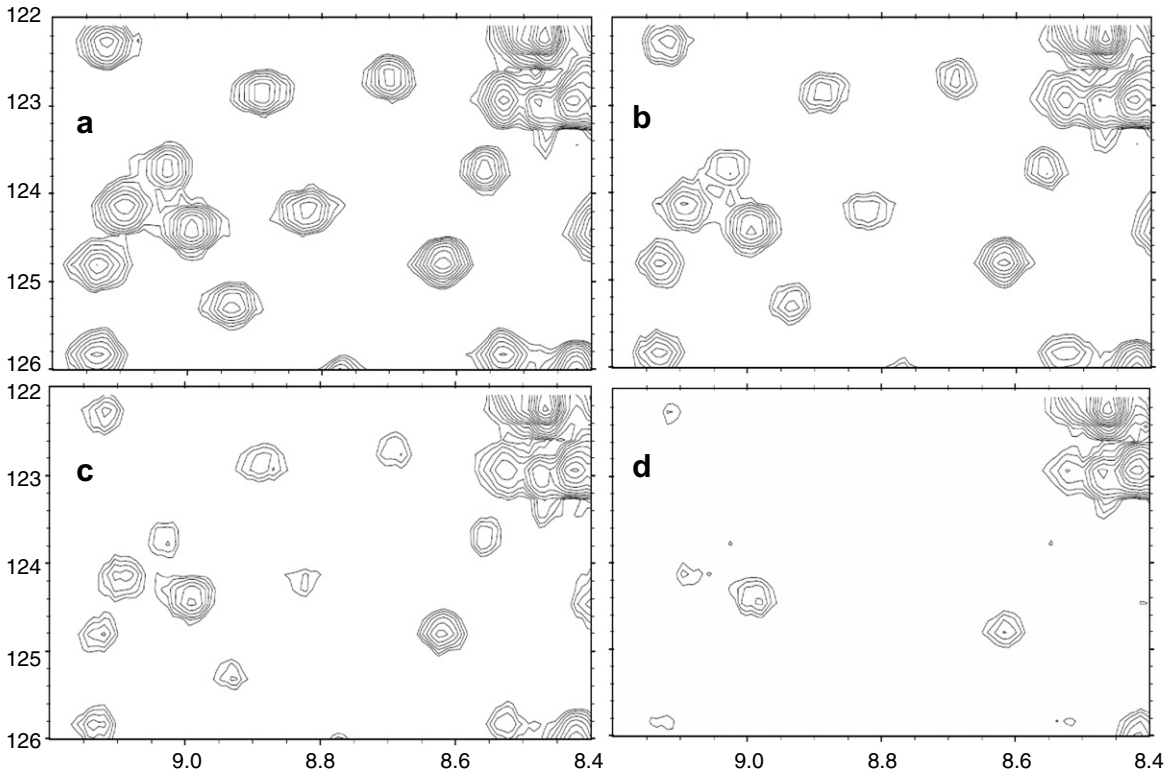

Fig. 2. ^{1}H-^{15}N HSQC NMR spectra of 1 mM uniformly ^{15}N-labeled syt1C2A in the presence of POPC:POPS vesicles at total lipid concentrations of (a) 25, (b) 35, (c) 50, and (d) 75 mM. All contour plots are scaled to the same relative amplitude.

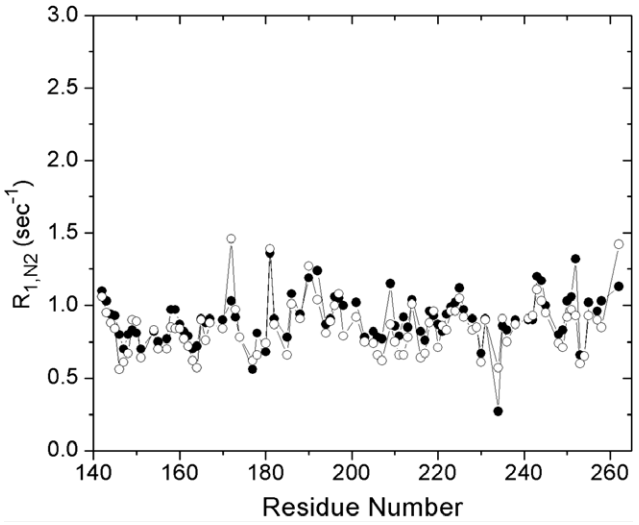

Fig. 3. ^{1}H spin-lattice relaxation rate constants $1/T_{1H}$ as a function of residue number for amide protons obtained for 1.2 mM C2A domain at pH 5.0 and 298 K in the calcium bound form under 10 atm N_2. Open circles represent data obtained in solution with no phospholipid, and filled circles correspond to data obtained with 25 mM phospholipid vesicles POPC:POPS (95:5).

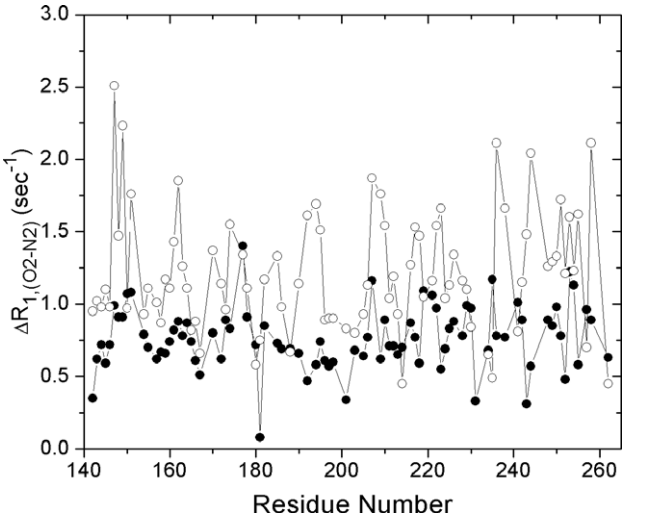

Fig. 4. Paramagnetic contributions to the ^{1}H spin-lattice relaxation rate constants induced by 10 atm oxygen as a function of residue number for 1.2 mM C2A domain at pH 5.0 and 298 K in the presence and absence of 25 mM POPC:PS (95:5). The open symbols represent the oxygen contribution to the relaxation rate for the protein in solution and the solid symbols represent the oxygen contribution for the protein in equilibrium with membranes where 5% of the protein is membrane bound protein.

Oxygen concentrations are higher in the membrane hydrocarbon than in the aqueous phase, and protein association with the membrane might be expected to result in an enhanced paramagnetic effect due to oxygen, particularly for those regions inserted into the membrane interior. However, the results shown in Fig. 4 clearly indicate that this is not the case, and the lipid binding region shown in Fig. 5b (which includes L1 and L3), shows no significant difference in oxygen enhancement relative to other regions of the protein.

A reasonable explanation for these results is that there is a dramatic change in spin dynamics that takes place when the protein associates with the bilayer. For the solution phase case, the proton-proton cross-relaxation rate is on the order of or less than the proton spin-lattice relaxation rate. As a result, there are significant differences detected in the paramagnetic contributions to different protons at different sites in the protein. Of course, the

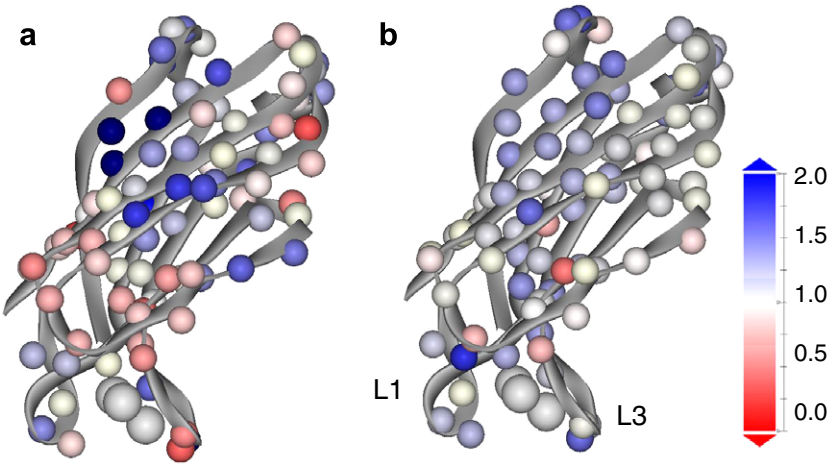

Fig. 5. A plot of the data in Fig. 4 on the structure of the synaptotagmin C2A domain (PDB ID: 1BYN) with the amid protons shown in a space filling representation for (a) the protein in solution, and (b) the protein in the presence of PC:PS lipid bilayers. The relaxation rate enhancements vary from 0.01 to 2.5 s^{-1}. The smallest rate enhancements are shown in red (0.1–1.0 s^{-1}), the largest rate enhancements are shown in blue (1.0–2.5 s^{-1}). The first and third calcium binding loops (L1 and L3) penetrate the bilayer.

intramolecular proton-proton coupling is not zero because nuclear Overhauser (NOE) effects can be measured and used to establish structural restraints; however, the cross-relaxation rate constants for the protein in solution are not so large that all protons have the same values of the spin-lattice relaxation rate or the same paramagnetic enhancement. For the membrane-bound protein, the rotational correlation time is estimated to be slower by approximately a factor of a thousand, and the membrane bound environment results in spin dynamics that approach that in a solid. The ^1H dipole-dipole couplings are still largely averaged by rotation, but the slow reorientation substantially increases the intra and intermolecular proton-proton cross-relaxation rates approximately in the ratio of the correlation time changes. Therefore, for the membrane-bound protein, the protons are strongly-coupled to each other. If we assume a van der Waals contact distance of 2.2 Å and a rotational correlation time of 10 μs for the membrane-bound protein, the cross-relaxation rate constant is approximately 5000 s^{-1}, which will rapidly bring the protein spins to the same spin temperature when bound to the membrane. For the membrane-bound protein, the relaxation rate constant for protons that are accessible to oxygen is increased; however, the differences associated with different accessibility that are apparent in the solution phase data are suppressed by the rapid spin diffusion within the slowly rotating membrane-bound spin system. The fast relaxation of one spin is distributed to nearly all spins, which dilutes the magnitude of the detectable change significantly. Because of this rapid internal spin diffusion, the overall effect is to make the relaxation effects of the oxygen on the protein protons look similar among all protons including the internal or non-surface protein spins where the oxygen effects would normally be small.

A second effect of the slow rotational reorientation time of the lipid-bound protein might be significant intermolecular coupling between the protein protons and the lipid protons. For protons that are magnetically in contact with the lipid pool, the effect would be to transfer relaxation effects from the protein protons into the large lipid-proton population and dilute the local effects of the paramagnetic oxygen further. The intermolecular cross-relaxation rate constant is difficult to estimate accurately because the lipid proton dynamics adjacent to the protein that control the intermolecular cross-relaxation rate are not accurately known. However, this effect is consistent with the reduction in average protein proton relaxation rate apparent in Fig. 4. We note that the protein–lipid cross-relaxation may affect the protein–proton paramagnetic effects in either direction. If the lipid protons are rapidly relaxed by a high concentration of oxygen in the lipid phase, then the lipid-protein coupling will enhance the proton relaxation rate constants for protein protons. If the lipid protons relax more slowly than the protein protons, the lipid-protein coupling will decrease the apparent protein–proton relaxation rate constant. The membrane-bound effects on the relaxation rate constants derive from the slow reorientational motion that significantly enhances the cross-relaxation rate among protons. The cross-relaxation effects may be largely eliminated in experiments of this class by studying heavily deuterated protein, which may not be practical in vivo.

In summary, the relatively high resolution provided by spin-lattice relaxation rate constant measurements in protein solutions is lost when the protein binds to a bilayer vesicle with slow rotational correlation time. This loss of relaxation enhancement resolution derives from a large increase in the intramolecular proton cross-relaxation rates and possibly intermolecular cross-relaxation rates that equalize the proton relaxation and suppress the local relaxation rate differences induced by diffusing paramagnets.

Acknowledgments

This work was supported by NIH Grants GM062305 (to D.S.C.) and NIBIB2805 (to R.G.B.).

References

[1] J.P. DiNitto, T.C. Cronin, D.G. Lambright, Membrane recognition and targeting by lipid-binding domains, Sci. STKE 2003 (2003) re16.
[2] G.E. Fanucci, D.S. Cafiso, Recent advances and applications of site-directed spin labeling, Curr. Opin. Struct. Biol. 16 (2006) 644–653.
[3] E.A. Nalefski, J.J. Falke, Location of the membrane-docking face on the Ca+2-activated c2 domain of cytosolic phospholipase A2, Biochemistry 37 (1998) 17642–17650.
[4] S. Malkova, F. Long, R.V. Stahelin, S.V. Pingali, D. Murray, W. Cho, M.L. Schlossman, X-ray reflectivity studies of cPLA2α-C2 domains adsorbed onto Langmuir monolayers of SOPC, Biophys. J. 89 (2005) 1861–1873.
[5] L.K. Tamm, S.A. Tatulian, Infrared spectroscopy of proteins and peptides in lipid bilayers, Q. Rev. Biophys. 30 (1997) 365–429.
[6] G. Esposito, A.M. Lesk, H. Molinari, A. Motta, N. Niccolai, A. Pastore, Probing protein structure by solvent perturbation of nuclear magnetic resonance spectra. Nuclear magnetic resonance spectral editing and topological mapping in proteins by paramagnetic relaxation filtering, J. Mol. Biol. 224 (1992) 659–670.
[7] G. Esposito, A.M. Lesk, H. Molinari, A. Motta, N. Niccolai, A. Pastore, Probing protein structure by solvent perturbation of NMR spectra. II. Determination of surface and buried residues in homologous proteins, Biopolymers 33 (1993) 839–846.

[8] G. Hernandez, C.L. Teng, R.G. Bryant, D.M. LeMaster, O2 penetration and proton burial depth in proteins: applicability to fold family recognition, J. Am. Chem. Soc. 124 (2002) 4463–4472.
[9] P.A. Luchette, R.S. Prosser, C.R. Sanders, Oxygen as a paramagnetic probe of membrane protein structure by cysteine mutagenesis and (19)F NMR spectroscopy, J. Am. Chem. Soc. 124 (2002) 1778–1781.
[10] H. Molinari, G. Esposito, L. Ragona, M. Pegna, N. Niccolai, R.M. Brunne, A.M. Lesk, L. Zetta, Probing protein structure by solvent perturbation of NMR spectra: the surface accessibility of bovine pancreatic trypsin inhibitor, Biophys. J. 73 (1997) 382–396.
[11] N. Niccolai, A. Ciutti, O. Spiga, M. Scarselli, A. Bernini, L. Bracci, D. Di Maro, C. Dalvit, H. Molinari, G. Esposito, P.A. Temussi, NMR studies of protein surface accessibility, J. Biol. Chem. 276 (2001) 42455–42461.
[12] N. Niccolai, R. Lampariello, L. Bovalini, M. Rustici, P. Mascagni, P. Martelli, Solvent spin-labelling for investigating the interaction of biological ligands with macromolecules. A 1H paramagnetic relaxation study, Biophys. Chem. 38 (1990) 155–158.
[13] N. Niccolai, C. Rossi, G. Valensin, P. Mascagni, W.A. Gibbons, An investigation of the mechanisms of nitroxide-induced proton relaxation enhancements in biopolymers, J. Phys. Chem. 88 (1984) 5689–5692.
[14] N. Niccolai, R. Spadaccini, M. Scarselli, A. Bernini, O. Crescenzi, O. Spiga, A. Ciutti, D. Di Maro, L. Bracci, C. Dalvit, P.A. Temussi, Probing the surface of a sweet protein: NMR study of MNEI with a paramagnetic probe, Protein Sci 10 (2001) 1498–1507.
[15] G. Pintacuda, G. Otting, Identification of protein surfaces by NMR measurements with a pramagnetic Gd(III) chelate, J. Am. Chem. Soc. 124 (2002) 372–373.
[16] R.S. Prosser, P.A. Luchette, P.W. Westerman, Using O2 to probe membrane immersion depth by 19F NMR, Proc. Natl. Acad. Sci. USA 97 (2000) 9967–9971.
[17] R.S. Prosser, P.A. Luchette, P.W. Westerman, A. Rozek, R.E. Hancock, Determination of membrane immersion depth with O(2): a high-pressure (19)F NMR study, Biophys. J. 80 (2001) 1406–1416.
[18] C.-L. Teng, R.G. Bryant, Experimental measurement of nonuniform dioxygen accessibility to ribonuclease A surface and interior, J. Am. Chem. Soc. 122 (2000) 2667–2668.
[19] N. Zhou, P. Mascagni, W. Gibbons, N. Niccolai, C. Rossi, H. Wyssbrod, Confirmation of the solution structure of tyrocidine A using perturbation of proton relaxation rates by nitroxide spin labels, J. Chem. Soc. Perkin Trans. 2 (1985) 581–587.
[20] W.K. Subczynski, J.S. Hyde, The diffusion-concentration product of oxygen in lipid bilayers using the spin-label T1 method, Biochim. Biophys. Acta 643 (1981) 283–291.
[21] D. Marsh, B.G. Dzikovski, V.A. Livshits, Oxygen profiles in membranes, Biophys. J. 90 (2006) L49–L51.
[22] J. Bai, E.R. Chapman, The C2 domains of synaptotagmin-partners in exocytosis, Trends Biochem. Sci. 29 (2004) 143–151.
[23] T.W. Koh, H.J. Bellen, Synaptotagmin I, a Ca2+ sensor for neurotransmitter release, Trends Neurosci. 26 (2003) 413–422.
[24] A.A. Frazier, C.R. Roller, J.J. Havelka, A. Hinderliter, D.S. Cafiso, Membrane-bound orientation and position of the synaptotagmin I C2A domain by site-directed spin labeling, Biochemistry 42 (2003) 96–105.
[25] A.A. Frazier, M.A. Wisner, N.J. Malmberg, K.G. Victor, G.E. Fanucci, E.A. Nalefski, J.J. Falke, D.S. Cafiso, Membrane orientation and position of the C2 domain from cPLA2 by site-directed spin labeling, Biochemistry 41 (2002) 6282–6292.
[26] K.G. Victor, D.S. Cafiso, Location and dynamics of basic peptides at the membrane interface: electron paramagnetic resonance spectroscopy of tetramethyl-piperidine-*N*-oxyl-4-amino-4-carboxylic acid-labeled peptides, Biophy. J. 81 (2001) 2241–2250.
[27] C.L. Teng, B. Hinderliter, R.G. Bryant, Oxygen accessibility to ribonuclease a: quantitative interpretation of nuclear spin relaxation induced by a freely diffusing paramagnet, J. Phys. Chem. A 110 (2006) 580–588.